

LWIR NUC Using an Uncooled Microbolometer Camera

Joe LaVeigne^a, Greg Franks^a, Kevin Sparkman^a,
Marcus Prewarski^a, Brian Nehring^a, Steve McHugh^a

^aSanta Barbara Infrared, Inc., 30 S. Calle Cesar Chavez, #D, Santa Barbara, CA 93103

ABSTRACT

Performing a good non-uniformity correction is a key part of achieving optimal performance from an infrared scene projector. Ideally, NUC will be performed in the same band in which the scene projector will be used. Cooled, large format MWIR cameras are readily available and have been successfully used to perform NUC, however, cooled large format LWIR cameras are not as common and are prohibitively expensive. Large format uncooled cameras are far more available and affordable, but present a range of challenges in practical use for performing NUC on an IRSP. Santa Barbara Infrared, Inc. reports progress on a continuing development program to use a microbolometer camera to perform LWIR NUC on an IRSP. Camera instability and temporal response and thermal resolution are the main difficulties. A discussion of processes developed to mitigate these issues follows.

Keywords: Scene Projection, LFRA, Mirage XL, LWIR, NUC, microbolometer, IRSP

1. INTRODUCTION

Non-uniformity correction (NUC) is important in the preparation of an infrared scene projector (IRSP) for projecting high fidelity images. A good NUC must be performed in the same response band as the sensor it is going to test. In the past, most LWIR NUCs have been performed using a cooled LWIR camera. While high performance cameras in the MWIR portion of the spectrum are fairly common and reasonably priced, cooled large format LWIR cameras are relatively expensive. Large format uncooled cameras are far more available and affordable, but present a range of challenges in practical use for performing NUC on an IRSP. In this paper, progress made towards using an uncooled microbolometer camera to perform NUC on an IRSP is described.

The IRSP used in this study was a Santa Barbara Infrared MIRAGE XL system^[1] with a 1024x1024 array capable of producing apparent temperatures of over 550K in the 8-12 micron band. (This corresponds approximately to a 700 K MWIR apparent temperature given the spectral output curve of the array.) The specific camera used in these experiments was a FLIR Photon 640 with a standard 25 mm f/1.4 lens. The focal plane array (FPA) has a pixel pitch of 25 μm and a NE Δ T of \sim 100 mK when coupled with the f/1.4 lens used. The as-manufactured near focus distance of the camera and lens combination was 2 meters. To focus on the array at shorter distances, a custom spacer was added between the camera and lens, which reduced the near focus distance to approximately 20 cm.

2. CAMERA CHARACTERIZATION

The most challenging aspect of any NUC process is developing a good understanding of the response of the camera being used. Most commercial cameras currently on the market produce excellent imagery for human viewing. However, a careful examination of the radiometric data collected from the camera is necessary for NUC measurements. Specific methods of data collection can be more prone to artifacts than others. For example, sparse grid measurements are susceptible to errors introduced by bad pixel replacement algorithms used in most cameras today. For sparse grid

measurements a single emitter will illuminate only a few camera pixels with a significant amount of radiance. If one of those pixels is bad, a replacement algorithm will almost certainly provide radiometrically incorrect data, although the image will certainly be more pleasing to the eye than one with a missing or stuck-on pixel. For these reasons, it is vital to disable any on-camera replacement algorithms and proceed with a raw output of the camera. Bad camera pixels can be found during camera calibration and appropriate measures taken to deal with any data corrupted by the bad camera pixels.

Microbolometer cameras have several distinct differences from cooled IR cameras typically used for NUC. First, they are significantly lower in price, which was the motivation for the work described here. Other features are they are uncooled, there is no gating (they are always integrating) and the pixels have a limited temporal response, they typically have more limited thermal resolution and a more limited dynamic range than a cooled camera. The uncooled nature of the camera leads in part to the lower thermal resolution due to increased background noise. It also leads to a more difficult problem of temporal drift. These three issues: Drift, temporal response and thermal resolution are the primary limitations in effectively using a microbolometer for NUC of an IRSP. Each will be discussed in more detail along with mitigation strategies.

2.1 Drift

The camera temperature tends to vary over time and this leads to an unstable background. This is particularly important in sparse grid measurements where the ratio of the collection area to the emitter area is rather high. The collection area for an emitter pixel in the sparse grid may cover 25 or more camera pixels. Furthermore, the emitter pixels usually map to a fraction of a camera pixel. This leads to the camera drift having greater than 100 times the impact on the sparse grid measurement than it would have on a flood scene of the same apparent temperature being calibrated. Figure 1 shows the result of a camera test where one frame was taken every 15 seconds for over an hour with the camera viewing an extended area blackbody set at 25 C. The plot is the average of a 20,000 pixel region of interest (ROI) in the center of the frame. There are long period variations that are likely due to the air conditioning cycle of the lab. There are also significant short period variations that occur even in the 15 seconds between the collected frames. Some of the variation can be removed by frequent dark subtraction. Performing frequent dark subtractions limits the effect of the background drift although it increases the test time. However, for very low signal measurements, even regular dark subtraction is not enough to produce an accurate result. Figure 1 also shows the average response of the same ROI while viewing a 25 C blackbody over the course of 10 seconds. There is significant variation even between frames. Figure 2 shows the previous response along with that from three other ROIs of approximately 100 pixels, each from within the larger ROI. Even in this short time frame, variations of over 1 count are recorded, and as shown by the smaller regions, much of this variation is coherent across the camera. Recall that 1 count is approximately 0.1 C, so a coherent variation of 1 count between the dark and light measurement would be the equivalent of a 25 count or 2.5 C error when summed over the region for a given emitter. This error is further multiplied by the area ratio of the camera pixel to emitter pixel, which in this case is approximately 5, leading to an effective 12.5C error at the emitter. This places a severe limit on the effectiveness of the NUC without some additional mitigation. Such a strategy involving collection reference data used to correct the drift is discussed in the next section.

2.2 Temporal Response

The temporal response of the microbolometer and its lack of gating control leads to another difficulty in collecting accurate radiometric data. The sensitivity of a microbolometer is determined in part by the thermal conductance of the legs; long thin legs with low thermal conductance lead to higher sensitivity. However, the frame rate is also affected by leg conductance with the lower conductance leading to lower frame rates. Microbolometers are typically designed to operate at video frame rates (~30 Hz). In order to maximize thermal sensitivity, they typically have time constants of around 30-50 ms. In order to achieve measurement errors of much less than 1%, a minimum settling time of 5-6 time constants must be used after any change in the commanded output. This adds a minimum wait of 0.2 to 0.3 seconds for each grid or dark frame to be collected. This is an important step to add to prevent artifacts, although it increases overall test time. Figure 3 shows the average response of approximately 600 camera pixels illuminated by a sparse grid as used in a typical NUC measurement. Although the responses shown in the figures are not well described by a simple exponential, the concept is the same and a significant wait time for camera settling is required for the output to approach its steady state. For the camera used here, this leads to a wait period of approximately 15 frames for the camera to stabilize before data collection could commence. Again, this leads to longer test times and furthermore limits the effectiveness of the dark subtraction due to the minimum time between data collections while waiting for the camera to settle.

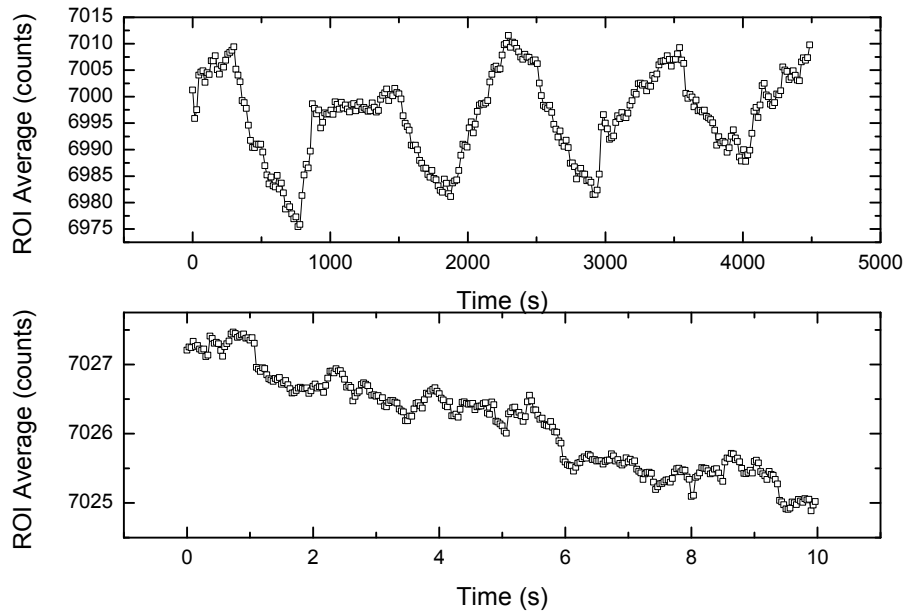


Figure 1. Camera Drift. This figure shows the average response of a 20,000 pixel ROI near the center of the camera while viewing a 25 C extended area blackbody. The upper plot shows a frame collected every 15 seconds for over an hour. The lower plot shows the same ROI over 10 seconds while operating at 30 Hz. The roughly periodic variation of the upper plot is due to the air conditioning cycle in the lab.

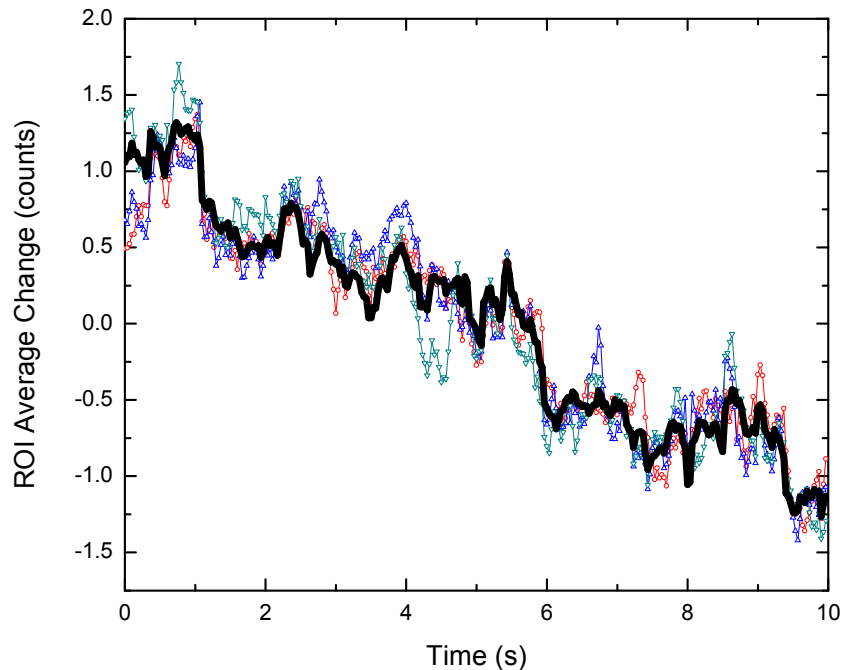


Figure 2. Camera drift. This figure shows camera drift of the 20,000 pixel ROI (bold line) as well as three ~100 pixel ROIs collected over the same period. The average of each ROI has been subtracted for easier comparison.

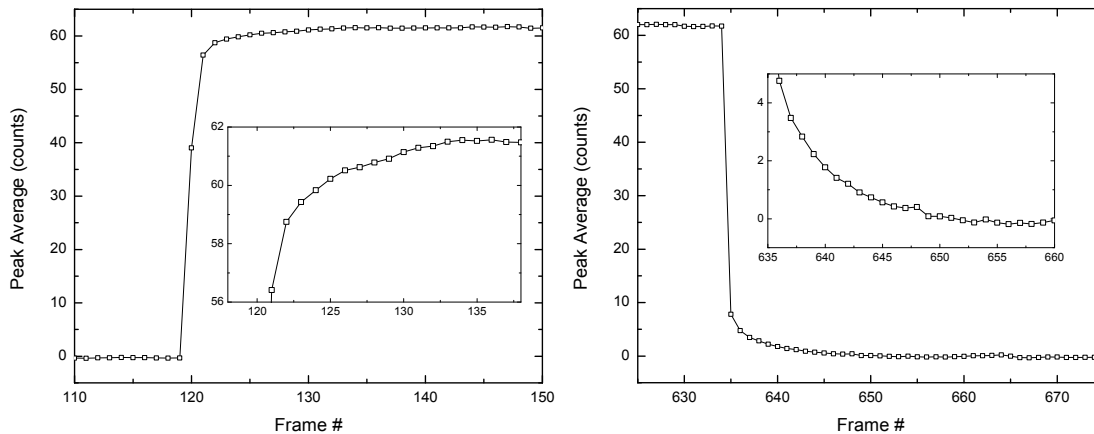


Figure 3. Temporal response of the camera. These plots show the temporal response of the camera. A sparse grid at 44000 drive was displayed and cycled on and off. The average response of the camera pixels located at the peaks of the grid is shown. The decay is consistent with a ~ 30 ms time constant. Approximately 15 frames or 0.5 seconds is required for the camera to settle after each transition.

2.3 Thermal Resolution

A final significant difference between the microbolometer and a typical cooled MWIR camera is its thermal resolution. A typical MWIR camera and lens would have a noise effective delta temperature (NE Δ T) of 10-15mK. The microbolometer and lens used in this test has a NE Δ T on the order of 100mK. This, combined with the residual drift problems, even after frequent background subtraction, limits the effectiveness of the microbolometer camera for NUC at low radiance.

3. NUC PROCESS

3.1 Camera Calibration

Camera calibration of the microbolometer was accomplished with an extended area differential blackbody (SBIR Model 11104). A multipoint piecewise linear calibration was used to convert recorded camera counts to radiance. One convenience of the lack of variable integration time is that the camera calibration is much simpler since calibrations for each different integration time are no longer used. During the calibration process pixels that are significantly outside the normal distribution are marked as bad pixels and subsequent data collected with those camera pixels is considered tainted and not used. To account for these emitter pixels, multiple data collections are run with different camera locations so that each emitter pixel is measured with all good camera pixels at least once. The camera used had a very small number of bad pixels and required only two passes to cover every emitter pixel. In the case of pixels with good data in both passes, the radiance values of the two passes were averaged.

3.2 Sparse Grid Radiance

The NUC procedure used in this paper is commonly referred to as a sparse grid measurement^[2,3]. In this method, a grid of emitter pixels is displayed, spaced far enough apart such that neighboring projected ON pixels are not interacting in the camera. Camera frames are captured and averaged and a region of interest is drawn around the emitter pixel and the energy collected by the camera in the region is summed and divided by the emitter pixel area to derive radiance for that pixel. Subsequent grids are displayed until all emitter pixels have been measured. A composite image of the emitter array radiance is then constructed from the individual grid measurements. As mentioned above, the camera is then moved and the process repeated to collect data from any emitter that was corrupted by a bad camera pixel. The process

is repeated for every drive level desired. Please see the references for more detail of the sparse grid method of correction.

3.3 Drift Correction

Correcting camera drift has been the most significant portion of this effort to date. Several algorithms and processes were attempted, but a final one derived from previous work at KHILS has proved to be the most effective. The basic premise is to use reference pixels to correct the collected radiance. The specific process is as follows: Prior to general data collection, radiance is collected from a series of reference grids with a pixel spacing different than that used in the general collection. For instance, if the general measurement will be performed with a spacing of 25 emitter pixels, the reference spacing might be 24 or 26 pixels. In each subsequent grid of general collection a fraction of the reference pixels are also illuminated. After collection of all of the general grids, the data from each grid is post-processed. The values of the reference pixels from each general grid and the initial reference grids are compared. Based on the ratio of the average radiance of these pixels from the reference grids and general grid, a correction factor is applied to the general grid to account for any drift in the camera. Figure 4 gives an example of the improvement achieved using drift correction. Figure 5 is an image of the remaining differences after drift correction has been applied.

3.4 NUC

The non-uniformity correction used in the IRSP is a piecewise linear correction with 16 segments. A lookup table for each segment contains gain and offset corrections for each pixel in the array. In the cases described here, the gain and offset for each pixel is derived from a linear interpolation of the radiance versus drive collected in the pre-NUC measurements.

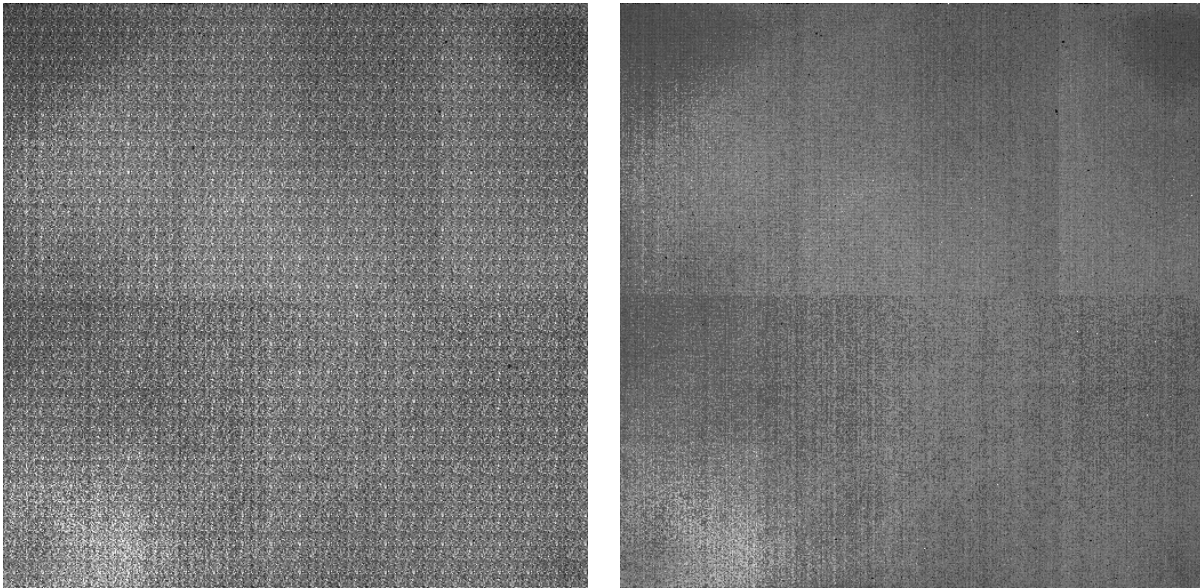


Figure 4. Results of drift correction. Pre-NUC composite images are shown from uniformity measurements taken with (right) and without (left) the camera drift correction algorithm. The NU without the drift correction algorithm is 36%, with drift correction it is 19%. Data was collected at a drive level of 40000. At this level, the error due to the camera drift is considerably larger than the non-uniformity in the array, as evident in the left image above.

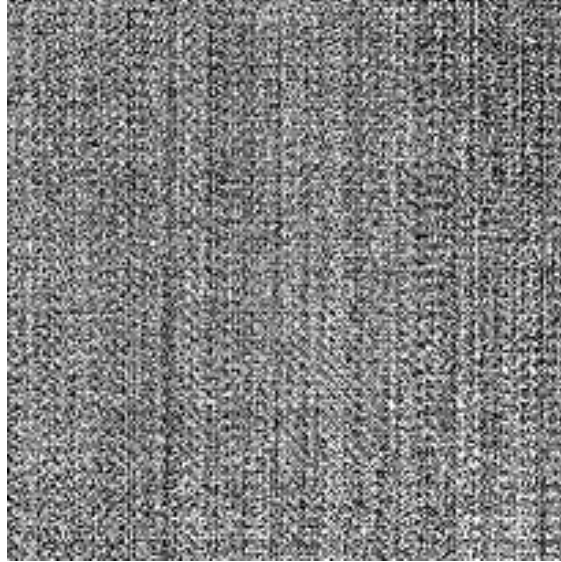


Figure 5. Residual error with drift correction. Difference between two consecutive uniformity measurements at 40000 drive with drift correction applied. Pattern noise due to drift is still a significant source of the lack of repeatability in the two measurements.

4. RESULTS

In general the results were reasonable with post-NUC non-uniformity considerably better than the pre-NUC. As discussed above, the residual non-uniformity after correction at lower radiance increased due to the limitations of the camera. Tables 1 and 2 show the pre and post NUC non-uniformity at three drive levels and the associated apparent temperatures. Figures 6, 7 and 8 shows pre and post NUC composite images taken at drive levels of 64000, 52000 and 40000 respectively. The NUC at the two higher drive levels shows significant improvements while that at 40000 shows a minor improvement at best.

Table 1 Pre NUC non-uniformity at three drive levels.

Drive	Radiance mean	Radiance sigma	Apparent Temp	NU
40000	0.0042	0.00080	305	0.191
52000	0.0186	0.00227	438	0.122
64000	0.0439	0.00291	575	0.066

Table 2 Post NUC non-uniformity at three drive levels.

Drive	Radiance mean	Radiance sigma	Apparent Temp	NU
40000	0.0036	0.00051	296	0.142
52000	0.0185	0.00022	437	0.012
64000	0.0383	0.00059	548	0.015

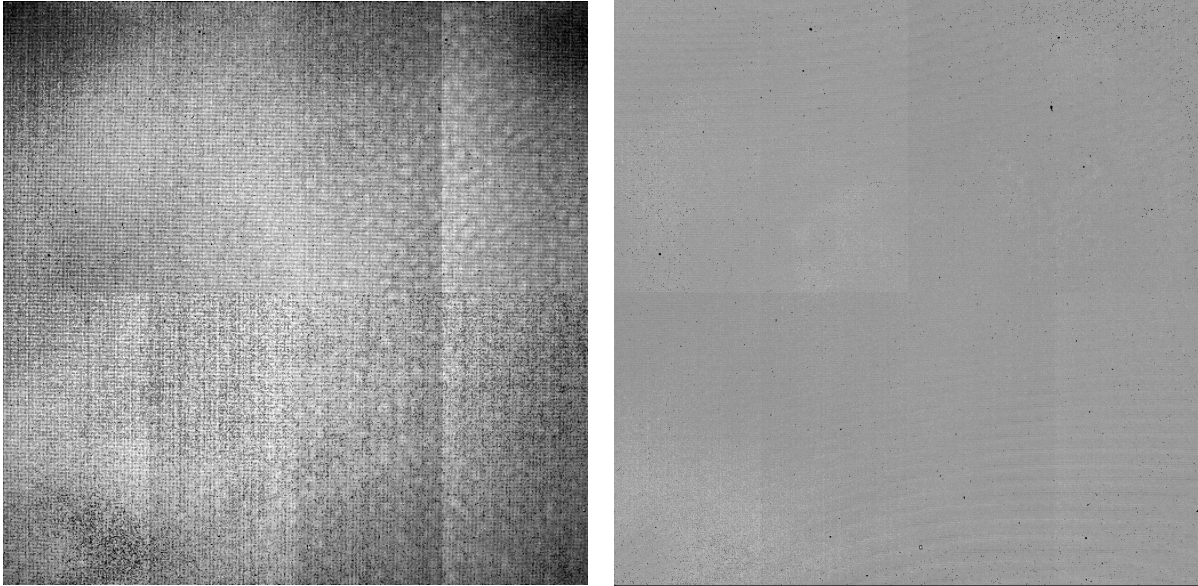


Figure 6. NUC results at 64000 Pre NUC and post NUC composite images at a drive of 64000. The apparent temperature is approximately 575K, pre NUC and 550K post NUC. The non uniformity before NUC is 6.5%, after NUC it is 1.5%.

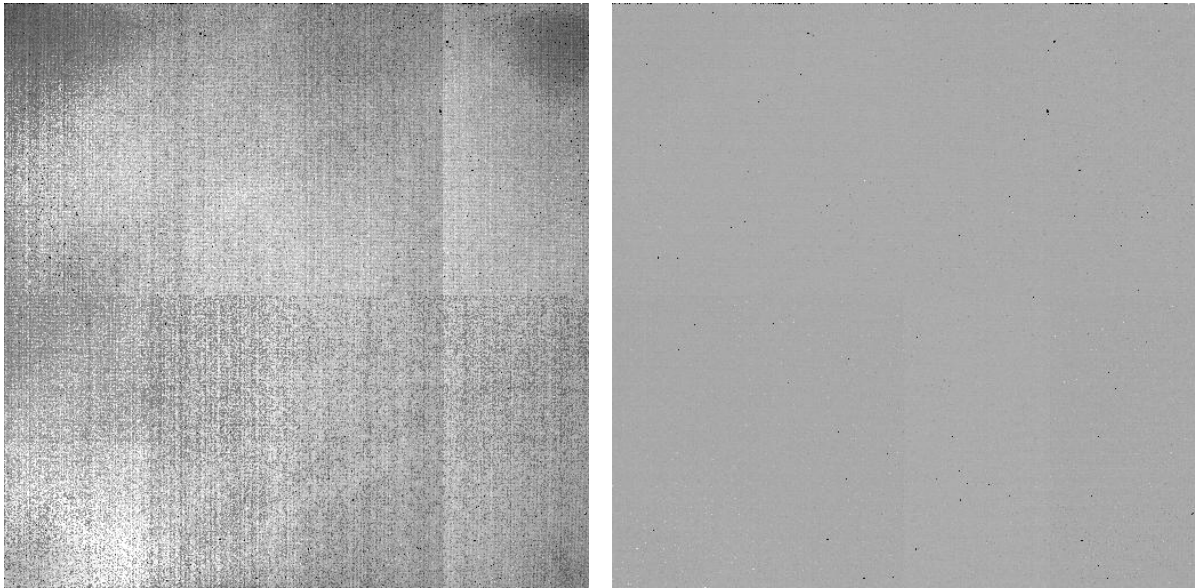


Figure 7. NUC results at 52000 Pre NUC and post NUC composite images at a drive of 52000. The apparent temperature is approximately 430K. The non uniformity before NUC is 12%, after NUC it is 1.25%.

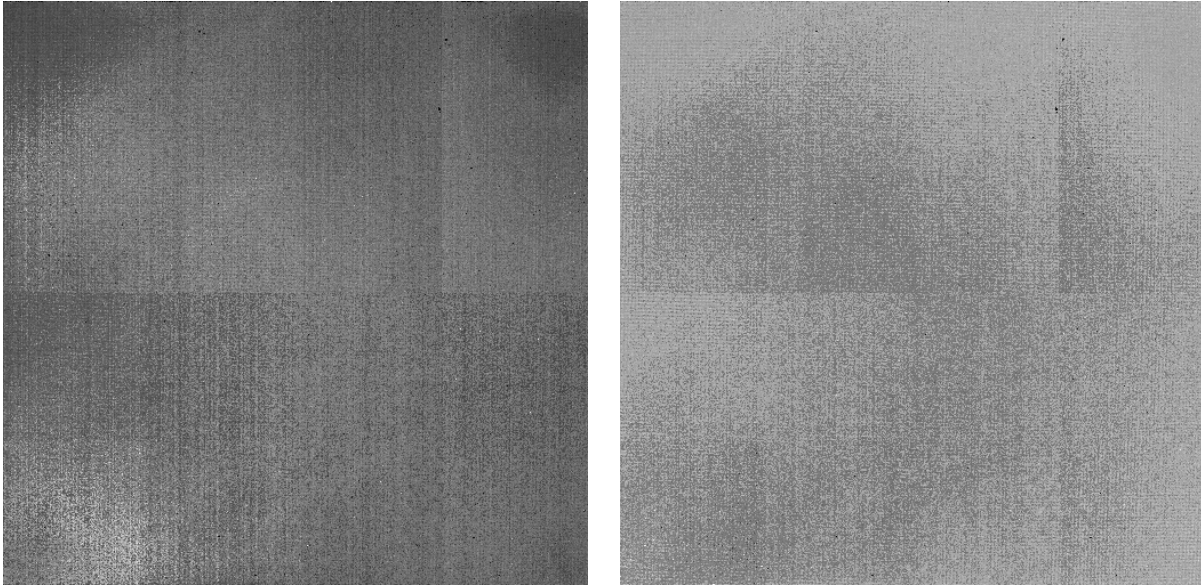


Figure 8. NUC results at 40000. Pre NUC and post NUC composite images at a drive of 40000. The apparent temperature is approximately 300K. The non uniformity before NUC is 19%, after NUC it is 14%.

4.1 Improvements

The progress to date described in these proceedings is part of a continuing effort to develop a low-priced LWIR NUC capability. These initial efforts focused on understanding the limits of the camera and most of the mitigation strategies involved minor changes to the NUC collection process and radiance calculation algorithms. Other steps are available to make further improvements. The limited thermal resolution was not thoroughly addressed in this paper. The most direct method for improving the resolution is to increase the number of photons to the camera pixels. First is to consider a custom lens. Moving to an $f/1$ lens would effectively halve the NEdT and hence improve the performance by a factor of two. Another possibility would be to change the effective emitter pixel size. The current setup is near optimal for viewing the entire array at once. However, it is possible to move closer to a 1:1 ratio of emitter to camera pixels. This would require tiling, as the camera would not be able to view the entire array at once, but it could result in a 4X increase in signal. These options were not among the first to be tried because they require the procurement of a custom lens. However, as the camera limits are approached, moving to a custom lens may be the most effective path to the goal of a reasonably priced LWIR NUC.

5. SUMMARY

Santa Barbara Infrared Inc., a HEICO company, has begun development of a LWIR NUC capability based on an uncooled microbolometer camera. Camera drift, thermal resolution and temporal response time all cause significant difficulties in the NUC process and require mitigation strategies. Drift correction, and additional waiting periods mitigate the worst of the camera drift and temporal response issues, yielding a process that is effective at moderately high to high (400-550K) apparent temperatures, reducing the NU from 12% to 1.2% and 6.6% to 1.4% respectively. However, the effectiveness remains limited below apparent temperatures of 40-50 C where the correction was only slightly improved from 19% to 14%. Additional modifications to the hardware and algorithm are planned to improve the capability at low temperatures and make the NUC process practical over the entire range of the infrared scene projectors.

REFERENCES

- [1] Oleson, J., et al " Large Format Resistive Array (LFRA) InfraRed Scene Projector (IRSP) Performance & Production Status," Proc. SPIE 6544, (2007).
- [2] Sieglinger, B., et al. " Array non-uniformity correction -- new procedures designed for difficult measurement conditions," Proc. SPIE 5092, (2003)
- [3] Sieglinger, B., et al., "Procedures and recent results for two-color infrared projection", Proc. SPIE 6208, (2006)